



Kingdom of Saudi Arabia
Imam Mohammad Ibn Saud Islamic University (IMSIU)
Faculty of Sciences – Department of Physics



Gravitational Lensing: A Window into Dark Matter Distribution

A graduation project submitted to the Department of Physics in partial fulfillment of the requirements for the degree of Bachelor of Science in Applied Physics

By

Abdulaziz Alhathlol

Supervisor

Prof. Ali Eid

IMSIU-Riyadh-KSA

May 2025

بِسْمِ اللَّهِ الرَّحْمَنِ الرَّحِيمِ

Acknowledgements

الشكر باللغة العربية.

أولاً وقبل كل شيء، أود أن أتقدم بخالص الشكر لله على منحي القوة والمثابرة لإكمال مشروع التخرج هذا.

وأتقدم بجزيل الشكر لمشرفي، الأستاذ الدكتور علي عيد، على توجيهاته القيّمة وتشجيعه ودعمه المتواصل طوال مدة هذا المشروع. فقد كانت معرفته العميقة وملاحظاته الثاقبة حاسمة في صياغة هذا العمل.

كما أود أن أشكر أعضاء هيئة التدريس والموظفين في قسم الفيزياء بجامعة الإمام محمد بن سعود الإسلامية على تهيئة بيئة أكاديمية داعمة، وعلى تزويدي بالموارد والمعرفة اللازمة للنمو كطالب وباحث.

إلى عائلتي، وخاصة والديّ، أشكركم على حبكم الراسخ ودعواتكم ودعمكم المستمر في كل خطوة من مسيرتي الأكاديمية. لقد منحني إيمانكم بي الدافع للمضي قدماً.

وأخيراً، أتقدم بجزيل الشكر لجميع أصدقائي وزملائي الذين شاركوني أفكارهم وملاحظاتهم وساندوني خلال اللحظات الصعبة من هذه الرحلة. لم يكن هذا الإنجاز ممكناً لولاكم.

شكراً لكم جميعاً.

English Acknowledgement.

First and foremost, I would like to express my deepest gratitude to Allah for granting me the strength and perseverance to complete this graduation project.

I am sincerely grateful to my supervisor, **Prof. Ali Eid**, for his invaluable guidance, encouragement, and continuous support throughout the duration of this project. His profound knowledge and insightful feedback were crucial in shaping this work.

I would also like to thank the faculty and staff of the **Department of Physics at Imam Mohammad Ibn Saud Islamic University** for creating a nurturing academic environment and for providing me with the resources and knowledge needed to grow as a student and researcher.

To my family, especially my parents, thank you for your unwavering love, prayers, and constant support in every step of my academic journey. Your belief in me gave me the motivation to keep pushing forward.

Finally, I extend my appreciation to all my friends and colleagues who shared ideas, provided feedback, and stood by me during the challenging moments of this journey. This achievement would not have been possible without you.

Thank you all.

Table of Contents

Chapter 1:	Introduction	1
Chapter 2:	General theory of Relativity	3
Chapter 3:	Gravitational lensing	8
3.1:	Gravitational lensing and its history.....	8
3.2:	Deflection of light.....	9
3.2.1:	In Newtonian theory.....	10
3.2.2:	In General theory of relativity.....	10
3.2.2.1:	The Schwarzschild lens.....	11
3.2.3:	Theoretical descriptions of some models.....	18
3.2.4:	Observations.....	23
3.2.4.1:	Photometry in astronomy.....	26
3.2.4.2:	Observation evidence.....	28
Chapter 4:	Discussion.....	34
4.1	Conclusion	33
4.2	Reference.....	34

List of Figures

Figure. 1. The GL geometry for a point-mass lens M at a distance D_d from an observer O . A source S at a distance D_s from O has angular separation β from the lens. A light ray from S which passes the lens at distance e is deflected by θ ; the observer sees an image of the source at angular position $\theta = \frac{\xi}{D_d}$.

الملخص

الملخص باللغة العربية.

يناقش هذا المشروع ظاهرة عدسة الجاذبية في إطار نظرية النسبية العامة لأينشتاين. تحدث عدسة الجاذبية عندما تحني جاذبية جسم ضخم مسار الضوء القادم من مصدر أبعد. يقدم هذا المشروع لمحة عامة عن تاريخ عدسة الجاذبية ونماذجها النظرية ورصدها، بما في ذلك وجهات النظر النيوتونية والنسبية. كما يتطرق بإيجاز إلى ملاحظات هذه الظاهرة الفلكية الرائعة. نناقش أيضًا أساسيات انحراف الضوء في نظرية النسبية العامة لأينشتاين ومعادلة العدسة الأساسية لكتلة نقطية. بعد ذلك، نُقدم نموذجين تمثيليين لتوزيع الكتلة، مثل نموذج نافارو- فرينك - وايت (NFW)، الذي يُستخدم غالبًا لوصف حالات المادة المظلمة، والكرة المتساوية الحرارة المفردة (SIS)، التي تُقارب كتلة المجرات الإهليلجية.

Abstract

English Abstract.

This project discusses the phenomenon of gravitational lensing in the framework of Einstein's general theory of relativity. Gravitational lensing occurs when the gravity of a massive object bends the path of light from a more distant source. This project provides an overview of history, theoretical models of gravitational lensing and observation, including Newtonian and relativistic perspectives. It also briefly touches upon observations of this fascinating astronomical phenomenon.

We also discuss the fundamentals of light deflection in Einstein's general theory of relativity and the basic lens equation for a point mass. Afterward, we introduce two representative mass-distribution models, such as the Navarro–Frenk–White (NFW) profile, often used to describe dark-matter halos, and the singular isothermal sphere (SIS), which approximates the mass of elliptical galaxies.

Chapter 1: Introduction

The concept of gravitational lensing has its roots in Einstein's general theory of relativity, which revolutionized our understanding of gravity. Unlike Newton's classical view of gravity as a force acting at a distance, Einstein described gravity as the curvature of spacetime caused by mass and energy. The idea that gravity could affect light isn't new. In 1704, Newton suggested that heavy objects might change the path of light. In 1783, John Michell talked about very massive objects that could trap light—an early version of what we now call black holes. Later, in 1796, Pierre-Simon Laplace had similar thoughts. In 1801, Soldner used Newton's laws to calculate how much light would bend near a massive object, but his answer was only half correct [1].

Einstein, in 1911, used his ideas to get the same result as Newton. But in 1915, after fully developing general relativity, he predicted that light would bend twice as much as Newton thought. This was proven in 1919, when Eddington's team saw starlight bending around the Sun during a solar eclipse. That discovery helped confirm Einstein's theory and sparked interest in gravitational lensing [2]. The first quantitative prediction of light deflection came from Soldner in 1801, by using Newtonian mechanics. However, his calculation only accounted for half the actual deflection observed. It wasn't until 1911 that Einstein, using his equivalence principle, arrived at the same Newtonian value for light bending. However, in 1915, with the full formulation of general relativity, he predicted the correct deflection angle which is twice the Newtonian estimate [1].

The first observational confirmation of gravitational lensing came several years later. During the solar eclipse of 1919, Eddington led an expedition to measure the deflection of starlight as it passed near the Sun. Eddington's team found that the amount of light deflection matched Einstein's predictions, providing strong evidence for general relativity and for the existence of gravitational lensing. This groundbreaking observation not only confirmed Einstein's theory but also opened the door for further study of gravitational lensing in the context of more distant and massive cosmic structures [2].

Since the 1980s, gravitational lensing has become an essential tool in astrophysics. The discovery of multiple lensing phenomena, such as Einstein rings, arc-shaped distortions in galaxy clusters, and microlensing events, has provided critical insights into the distribution of dark matter, the structure of the universe, and the nature of dark energy [1]. Gravitational lensing is generally classified into three main types: Strong lensing, Weak lensing and Microlensing

Moreover, strong and weak lensing provides a more comprehensive understanding of how gravitational lensing is used to study the structure and evolution of the universe.

Recently, Gravitational lensing is explained as the evidence of different astrophysical phenomena and theoretical models. For instance, Kormann et al. [3] studied gravitational lensing by elliptical mass. Navarro et al. [4] discussed the structure of cold dark matter halos and studied that density decreased with distance from center. Godani et al. [5] studied how light bends near charged wormholes and how photon spheres form rings around them. Furthermore, Gao et al. [6] investigated how adding a small extra distance-dependent term to standard black hole metrics changes the amount and behavior of strong gravitational lensing. Giani et al. [7] investigated how well certain scalar field models of dark energy match real observations from strong gravitational lensing.

In addition, Mehrotra et al. [8] simulated how light bends around a Schwarzschild black hole using images of different galaxy types as backgrounds. Heyrovsky et al. [9] found an exact formula for how light bends around ellipsoidal NFW dark matter halos and studied its lensing features. In addition, gravitational lensing has become one of the most powerful techniques for mapping the universe's large-scale structure [10].

This project is organized as follows. Chapter 2 discussed the short description of the general theory of relativity. Chapter 3 addresses gravitational lensing via different models. Chapter 4, remarkable conclusion.

Chapter 2: General theory of Relativity

2.1 CURVETURE AND MATTER

The General Theory of Relativity (GTR) is one of the most profound and elegant physical theories ever developed. Proposed by Einstein in 1915, it revolutionized our understanding of gravity by describing it not as a force, as in Newtonian mechanics, but as a manifestation of the curvature of spacetime caused by mass and energy.

Before GTR, Newton's law of universal gravitation provided the most successful description of gravity:

$$F = G \frac{m_1 m_2}{r^2} .$$

This equation describes a force acting instantaneously at a distance between two masses. However, it conflicts with special relativity, which requires that no information travel faster than the speed of light.

A major turning point occurred when Einstein, inspired by a thought experiment involving an accelerating elevator, realized that the effects of gravity and acceleration are locally indistinguishable. This insight, known as the equivalence principle, laid the foundation for GR.

In addition, Poincaré had already investigated the idea of gravitational waves propagating at the speed of light and speculated that relativity principles might apply to all physical laws. Moreover, it was Einstein who took the decisive steps toward a full gravitational theory compatible with special relativity.

In 1915, Einstein generalized special relativity to include non-inertial frames of reference. He used a Riemannian geometry as the mathematical foundation for his theory. This allowed him to describe spacetime as a four-dimensional manifold whose curvature is determined by the presence of mass and energy.

He used the linearized approximation of gravity (field in flat spacetime) to introduce the field equation:

$$R_{\mu\nu} = k T_{\mu\nu} .$$

where $R_{\mu\nu}$ is the covariant Ricci tensor while $R^{\mu\nu}$ is the contravariant. But this equation was not generally covariant; then he used Ricci scalar to achieve general covariance and conservation of energy-momentum.

Accordingly, Einstein field equations (EFE) become

$$R_{\mu\nu} - \frac{1}{2}Rg_{\mu\nu} = \frac{8\pi G}{c^4}T_{\mu\nu} .$$

These equations relate the geometry of spacetime (left-hand side) to the distribution of matter and energy (right-hand side). This equation looks like

Curvature = Matter

where curvature is a complicated function of the metric $g_{\mu\nu}$. The left-hand side takes the metric and computes a local measure of the curvature of spacetime. The right-hand side expresses how all the matter around sources the bending of spacetime. Briefly, matter tells spacetime how to curve.

2.2 Metric

The metric and geodesic postulates describe the behavior of clock, light, and internal particles in a curved spacetime. To apply these postulates, we must know the metric of the spacetime. Our final postulate for general relativity, the field equation, determines the metric. Loosely speaking, the equation determines the “shape “of a spacetime, how it is “curved “. There is a relationship between the motion of local inertial frames and the distribution of mass in a curved spacetime. Thus, there is a relationship between the metric of a space time and the distribution of mass in spacetime. The field equation gives this relationship. Schematically it reads:

[Quantity determined by metric] = [Quantity determined by mass/energy].

The geometry of GR is described by the metric tensor $g_{\mu\nu}$, which defines distances and angles in curved spacetime. The Christoffel symbols $\Gamma_{\mu\nu}^\lambda$ describe how coordinates change, and the Riemann curvature tensor $R_{\sigma\mu\nu}^\rho$ represent the intrinsic curvature:

$$R_{\sigma\mu\nu}^\rho = \partial_\mu \Gamma_{\nu\sigma}^\rho - \partial_\nu \Gamma_{\mu\sigma}^\rho + \Gamma_{\mu\lambda}^\rho \Gamma_{\nu\sigma}^\lambda - \Gamma_{\nu\lambda}^\rho \Gamma_{\mu\sigma}^\lambda .$$

Contracting it to give the Ricci tensor,

$$R_{\mu\nu} = R_{\mu\lambda\nu}^\lambda ,$$

and the Ricci scalar is defined by

$$R = g^{\mu\nu} R_{\mu\nu} .$$

These quantities are used in the EFE to describe how matter curves spacetime.

The cornerstones of general relativity depend on two main principles:

The first is the ***Principle of Covariance***: The equations of physics should be in a tensorial form, or equivalently “equations of physics should have the same form in all coordinate systems”.

The second is the ***principle of Equivalence***: On a local scale, without looking at other systems, it is impossible to distinguish between physical effects due to gravity and those due to acceleration (Inertia).

One of the most historic confirmations of Einstein's theory came in 1919, during a solar eclipse expedition led by Eddington. According to general relativity, light from distant stars passing near a massive object like the sun should follow a curved path due to the curvature of spacetime. Einstein had predicted that the sun would bend the light of stars behind it by approximately 1.75 arcseconds, this result is double that predicted by Newtonian gravity.

Eddington's team photographed the positions of stars near the sun during the eclipse. The comparison of the star positions during and after the eclipse confirmed that the light was indeed deflected by the amount Einstein predicted.

Also, GTR explains the anomalous procession of Mercury's perihelion (which Newtonian physics could not fully account), GTR precisely predicted the discrepancy observed in Mercury's orbit.

Meanwhile, unconfirmed predictions of general relativity such as Gravitational waves; Gravitational lenses; Singularity; Black holes and Wormholes; Hypersurfaces: Surface Layers, Boundary Layers, Null Surface; Thin/Thick Shell, Null Shell; Domain Wall; Bubble; Voids; Brane; Monopole; Dark energy and matter and so on.

In 1916, Schwarzschild found the first exact solution of the field equation. This solution describes the static and spherically symmetry spacetime in the vacuum $R_{\mu\nu} = 0$ around an object of mass M, described by the line element:

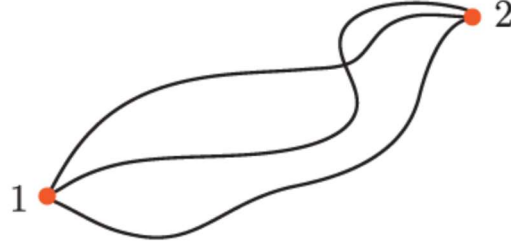
$$ds^2 = \left(1 - \frac{2GM}{c^2 r}\right) c^2 dt^2 - \left(1 - \frac{2GM}{c^2 r}\right)^{-1} dr^2 - r^2(d\theta^2 + \sin^2 \theta d\phi^2).$$

This is the spacetime around a black hole, or outside a spherical star.

This solution laid the groundwork for the concept of black holes, objects so dense that not even light can escape their gravitational pull, or outside a spherical star.

Furthermore, exact solutions such as the Reissner-Nordström (charged black holes) and Kerr (rotating black holes) metrics were discovered. These solutions have deep astrophysical implications, such as explaining quasars and active galactic nuclei and so on

To explain how space tells matter to move, suppose we have a curve spacetime, specified by a metric. How do particles move? For example, how does the moon move in the curves space created by the Earth? It's simplest to describe this in terms of the principle of least action. We consider all possible paths between two points:



The (relativistic) action for the particle is simply given by:

$$S = -mc \int_1^2 ds .$$

This doesn't quite yet look the usual integral over kinetic minus potential energy, but we will get there. Paths which minimize this action are called geodesics.

There are two types of equation of motion: Geodesic and Null Geodesic.

$$G^{\mu\nu} = kT^{\mu\nu} . \quad (2.1)$$

Where $k = -8\pi G/c^4$ is some coupling constant. Where G is a covariant form of the tensor (geometric quantity) and T is the energy momentum tensor (physical quantity). This looks plausible, because both $G^{\mu\nu}$ and $T^{\mu\nu}$ are symmetric, and $R_{;\mu}^{\mu\nu} = 0$ in agreement with $T_{;\mu}^{\mu\nu} = 0$. However, equation (2.1) does not reduce to Poisson's equation $\nabla^2 V = 4\pi G\rho$, in the Newtonian limit. In general, the field equation is described by

$$\mathbf{G} = -8\pi k\mathbf{T}.$$

Since $R^{\mu\nu}$ is symmetric and contains second derivatives of $g^{\mu\nu}$. However, $R^{\mu\nu}$ does not satisfy $R_{;\mu}^{\mu\nu} = 0$, and later in the same year he modified the equation to becomes

$$R^{\mu\nu} - \frac{1}{2}Rg^{\mu\nu} = kT^{\mu\nu} \quad (2.2)$$

where $R^{\mu\nu}$ is the contravariant Ricci tensor.

The left-hand side of this equation is the Einstein tensor $G^{\mu\nu}$, and we know from and $G_{;\mu}^{\mu\nu} = 0$, so equation (2.2) looks satisfactory in all respects. An alternative form for the field equations (2.2) is described by

$$R^{\mu\nu} = k(T^{\mu\nu} - \frac{1}{2}Tg^{\mu\nu}) . \quad (2.3)$$

where $T = T_{\mu}^{\mu}$ and $T^{\mu\nu}$ contains all forms of energy and momentum. For instance, if there is electromagnetic radiation present, then this must be included in $T^{\mu\nu}$. A region of

spacetime in which $T^{\mu\nu} = 0$, is called empty, and such a region is therefore not only devoid of matter, but of radiative energy and momentum also. It can be seen from equation (2.3) that the empty spacetime field equations are

$$R^{\mu\nu} = 0 . \quad (2.4)$$

Further support for the correctness of the field equations is given by comparing the equation of geodesic deviation with its Newtonian counterpart. With proper time τ as affine parameter, the geodesic deviation can be written in the form

$$\frac{D^2 \xi^\mu}{D\tau^2} + R^\mu_{\sigma\nu\rho} \xi^\nu \dot{x}^\sigma \dot{x}^\rho = 0$$

Where $\xi^\mu(\tau)$ is the small vector connecting corresponding points on neighboring geodesics. For comparison with its Newtonian counterpart, let us write this as

$$\frac{D^2 \xi^\mu}{D\tau^2} = -K^\mu_\nu \xi^\nu ,$$

where

$$K^\mu_\nu \equiv R^\mu_{\sigma\nu\rho} \dot{x}^\sigma \dot{x}^\rho = -R^\mu_{\sigma\nu\rho} \dot{x}^\sigma \dot{x}^\rho .$$

The corresponding situation in Newtonian gravitation theory is two particles moving under gravity on neighboring paths given by $\tilde{x}^i(t)$ and $x^i(t)$.

Afterward, Einstein introduced the cosmological constant Lambda (Λ) to maintain a static universe model. Therefore, the modified field equations can be written in this form

$$R_{\mu\nu} - \frac{1}{2} R g_{\mu\nu} + \Lambda g_{\mu\nu} = \frac{8\pi G}{c^4} T_{\mu\nu} .$$

In 1929, Hubble's investigated the idea of expanding universe according to this Λ . Accordingly, Einstein later called this as his biggest blunder. Moreover, later developments in relativistic cosmology, particularly the Friedmann-Lemaître-Robertson-Walker (FLRW) metric, allowed the modeling of a dynamic, expanding universe. These models provided a theoretical framework for the Big Bang theory.

Furthermore, gravitational waves, ripples in spacetime predicted by GR, were confirmed a century after the theory's inception. In 2015, the LIGO collaboration detected gravitational waves from a binary black hole merger, marking a new era in observational astrophysics. These discoveries validate one of GR's most exotic predictions and open avenues for probing the universe's most energetic events, such as neutron star mergers and black hole collisions. Despite its success, GR is not a complete theory of gravity. It is incompatible with quantum mechanics, and a viable quantum gravity theory remains elusive. Efforts such as string theory and loop quantum gravity aim to unify GR with quantum field theory.

Moreover, dark energy and dark matter, which dominate the universe's energy content, are not explained by GR. These mysteries hint at the need for a more comprehensive framework or extensions to GR.

Chapter 3: Gravitational lensing

3.1 Gravitational Lensing and its History

Gravitational lensing is a remarkable phenomenon predicted by Einstein's General Theory of Relativity (GR) in 1915. It describes the bending of light caused by the gravitational field of a massive object, such as a galaxy or black hole, that lies between a distant source and an observer. As the light passes near the massive object, the gravitational field warps the fabric of spacetime, causing the light to follow a curved path. This effect can lead to multiple images, distortions, and even rings of light, providing a powerful tool for observing distant cosmic objects and phenomena. The discovery and subsequent study of gravitational lensing has become integral to the field of modern astrophysics, enabling scientists to probe the universe in ways that were once unimaginable.

Gravitational lensing is generally classified into three main types, such as: Strong lensing (when a massive object creates highly visible distortions, such as multiple images or Einstein Rings. This effect is seen in massive galaxy clusters); Weak lensing (when distortions are subtle, requiring statistical analysis. It helps in mapping dark matter distribution); Microlensing (when a single star or compact object temporarily magnifies a background source. This technique is used to detect exoplanets and dark objects).

Recently, lensing effects have become crucial observational tools in modern astrophysics, offering insights into both visible and dark matter distributions in the universe.

Theoretical Prediction and Early History

The idea of gravitational lensing was first proposed by Einstein in 1915, shortly after he published his theory of general relativity. In general relativity, gravity is not described as a force, as in Newtonian physics, but as the result of the curvature of spacetime caused by the presence of mass and energy. This led to the realization that massive objects, such as stars or galaxies, could bend the path of light passing near them, much like a lens bends light in optical systems.

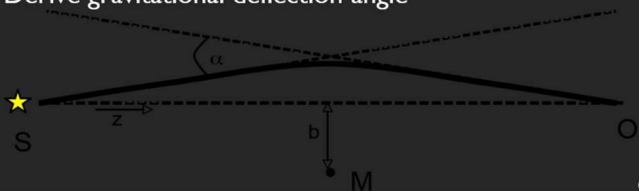
Einstein's original prediction was that the light from a star passing near the Sun would be deflected due to the Sun's gravitational field. He calculated that the amount of deflection would be small but measurable. Although the bending of light by gravity was a theoretical prediction, it was not immediately observable due to the complexity of detecting such subtle effects.

Afterward, the first observational confirmation of gravitational lensing came several years later. During the solar eclipse of 1919, Eddington led an expedition to measure the deflection of starlight as it passed near the Sun. Eddington's team found that the amount of light deflection matched Einstein's predictions, providing strong evidence for general relativity and for the existence of gravitational lensing. This groundbreaking observation not only confirmed Einstein's theory but also opened the door for further study of gravitational lensing in the context of more distant and massive cosmic structures.

3.2 Deflection of Light

When light from a distant galaxy passes near a massive object, like a galaxy cluster, that mass bends the fabric of spacetime, causing the light's path to curve. This bending can produce multiple apparent positions of the same background object, stretched arcs, or even complete rings when the alignment is just right. By observing how the light is distorted, astronomers can infer the distribution of both visible and dark matter in the lensing object.

Derive gravitational deflection angle



α from GR - just sketch elements here see e.g. Carroll for a complete treatment

Metric: $ds^2 = -(1 + 2\Phi)dt^2 + (1 - 2\Phi)(dx^2 + dy^2 + dz^2)$ Poisson Equation: $\nabla^2\Phi = 4\pi G\rho$

$\frac{d^2x^\mu}{d\lambda^2} + \Gamma^\mu_{\rho\sigma} \frac{dx^\rho}{d\lambda} \frac{dx^\sigma}{d\lambda} = 0$

Geodesic equation: $\frac{d\lambda^2}{d\lambda} + \Gamma^\mu_{\rho\sigma} \frac{dx^\rho}{d\lambda} \frac{dx^\sigma}{d\lambda} = 0$

Null path condition: $g_{\mu\nu} \frac{dx^\mu}{d\lambda} \frac{dx^\nu}{d\lambda} = 0$

Solve for photon path assuming that deflection is small so can treat as a small perturbation and integrate along the undeflected path to obtain Deflection angle:

$$\hat{\alpha} = 2 \int \nabla_\perp \Phi ds$$

3.2.1 In Newtonian theory

Newton wondered whether light, in the form of particles, would be bent due to gravity. The Newtonian prediction for light deflection refers to the amount of deflection a particle would feel under the effect of gravity, and therefore one should read "Newtonian" in this context as

the referring to the following calculations and not a belief that Newton held in the validity of these calculations.

For a gravitational point-mass lens of mass M , a particle of mass m feels a Force.

Using Newtonian gravity, the deflection angle of light passing by a massive body (assuming light behaves like a particle) is given by:

$$\theta = \frac{2GM}{c^2 r}$$

where G is the gravitational constant, M is the mass of the lensing object, c is the speed of light and r is the impact parameter (closest approach of light to the mass). The result is half of the correct value predicted by General relativity.

3.2.2 In General Theory of Relativity

Gravitational lensing is based on Einstein's general theory of relativity, which changed how we think about gravity. Instead of seeing gravity as a force (like Newton did), Einstein explained it as the bending of space and time caused by mass and energy. The idea that gravity could affect light isn't new. In 1704, Newton suggested that heavy objects might change the path of light. In 1783, Michell talked about very massive objects that could trap light an early version of what we now call black holes. Later, in 1796, Laplace had similar thoughts. In 1801, Soldner used Newton's laws to calculate how much light would bend near a massive object, but his answer was only half correct.

Einstein, in 1911, used his ideas to get the same result as Newton. But in 1915, after fully developing general relativity, he predicted that light would bend twice as much as Newton thought.

$$\theta = \frac{4GM}{c^2 r}$$

where G is the gravitational constant, M is the mass of the lensing object, c is the speed of light and r is the impact parameter (closest approach of light to the mass).

This was proven in 1919, when Eddington's team saw starlight bending around the Sun during a solar eclipse. That discovery helped confirm Einstein's theory and sparked interest in gravitational lensing. In general relativity, light follows the curvature of spacetime, hence when light passes around a massive object, it is bent. This means that the light from an object on the other side will be bent towards an observer's eye, just like an ordinary lens. In general relativity the path of light depends on the shape of space (i.e. the metric). The gravitational attraction can be viewed as the motion of undisturbed objects in a background curved *geometry* or alternatively as the response of objects to a *force* in a flat geometry. We will discuss a brief basic relation between lens mass and angular separation.

3.2.2.1 The Schwarzschild lens

By solving the geodesic equation for light in the Schwarzschild metric, Einstein derived the correct deflection angle. The Schwarzschild metric described by

$$ds^2 = \left(1 - \frac{2GM}{rc^2}\right) c^2 dt^2 - \left(1 - \frac{2G}{rc^2}\right)^{-1} dr^2 - r^2(d\theta^2 + \sin^2 \theta d\phi^2) .$$

Einstein's deflection law. One of the early tests of General Relativity concerned light deflection by the Sun. General Relativity predicts that a light ray which passes by a spherical body of mass M at a minimum distance ξ is deflected by the Einstein angle

$$\hat{\alpha} = \frac{4GM}{c^2 \xi} = \frac{2R_s}{\xi} , \quad (3.1)$$

provided the impact parameter ξ is much larger than the corresponding Schwarzschild radius

$$R_s = \frac{2GM}{c^2} . \quad (3.2)$$

The validity of (3.1) in the gravitational field of the Sun has been confirmed with radio-interferometric methods with an uncertainty of less than 1%. To demonstrate the effect of a deflecting mass, the simplest gravitational lensing (GL) configuration is plotted in figure 1.

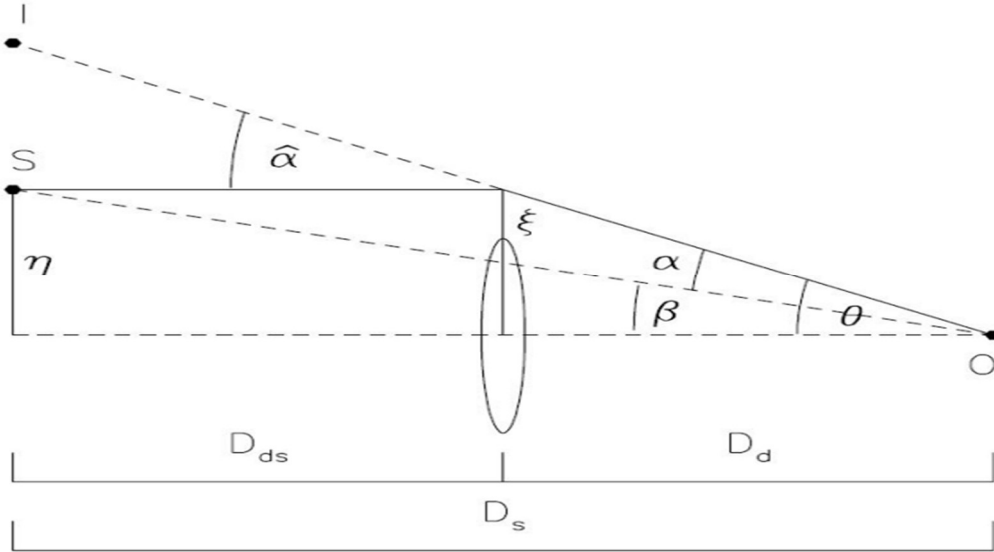
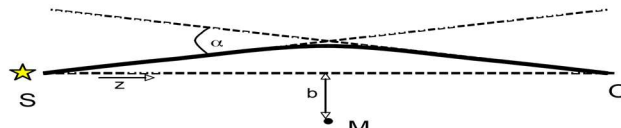


Figure. 1. The GL geometry for a point-mass lens M at a distance D_d from an observer O . A source S at a distance D_{ds} from O has angular separation β from the lens. A light ray from S which passes the lens at distance e is deflected by α ; the observer sees an image of the source at angular position $\theta = \frac{\xi}{D_d}$.

A point mass M is located at a distance D_d . According to General Relativity, a static spherical body with Schwarzschild radius R_s has a geometrical radius R larger than $(9/8)R_s$

while for a static black hole, $R = R_s$. Nevertheless, in lens theory the term "point mass" is used whenever one is concerned with light rays deflected with impact parameters $\xi \gg R_s$ by a spherical object, irrespective of the (unobservable) behavior of light rays with $\xi \sim R_s$.

Example: Point mass



Start here:

$$\hat{\alpha} = 2 \int \nabla_{\perp} \Phi \, ds \qquad \nabla^2 \Phi = 4\pi G \rho$$

Poisson eq. gives potential:

$$\Phi(r) = -\frac{GM}{r} = -\frac{GM}{(b^2 + z^2)^{1/2}} \qquad \nabla_{\perp} \Phi(r) = \frac{\partial \Phi}{\partial b} = -\frac{GMb}{(b^2 + z^2)^{3/2}}$$

Deflection angle follows:

$$\begin{aligned} \hat{\alpha} &= 2 \int \nabla_{\perp} \Phi(r) \, dz \\ &= 2 \int_{-\infty}^{\infty} dz \frac{GMb}{(b^2 + z^2)^{3/2}} \\ &= \frac{2GM}{b} \int_{-\infty}^{\infty} \frac{dx}{(1 + x^2)^{3/2}} \\ &= \frac{4GM}{b} \end{aligned} \qquad \boxed{\hat{\alpha} = \frac{4GM}{b}}$$

Example: Point mass lens

$$\left. \begin{aligned} \hat{\alpha} &= \frac{4GM}{c^2 |\xi|} \\ \alpha(\theta) &= \frac{D_{LS}}{D_s} \hat{\alpha}(\theta) \end{aligned} \right\} \alpha(\theta) = \frac{4GM}{c^2} \frac{D_{LS}}{D_s D_L} \frac{\theta}{|\theta|^2}$$

Einstein Radius $\theta_E = \sqrt{\frac{4GM}{c^2} \frac{D_{LS}}{D_s D_L}}$

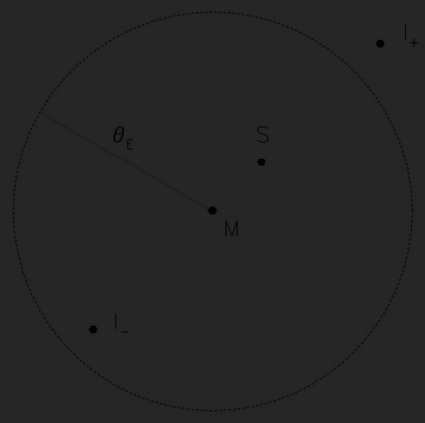
Lens equation $\beta = \theta - \theta_E^2 \frac{\theta}{|\theta|^2}$

$\beta > \theta_E$ source weakly lensed one weakly distorted image

$\beta < \theta_E$ source strongly lensed and multiple images

Two solutions $\theta_{\pm} = \frac{1}{2} \left(\beta \pm \sqrt{\beta^2 + 4\theta_E^2} \right)$

Symmetry forces source, lens and images to lie on same line



The source is at a distance D_s from the observer, and its true angular separation from the lens M is β , the separation which would be observed in the absence of lensing. Due to the symmetry of the Schwarzschild lens, any light ray traveling from the source to the observer is confined to the plane spanned by source, lens, and observer. Therefore, instead of the two-dimensional separation vector of light rays from the lens, a one-dimensional treatment suffices here. Note that in the case $\beta = 0$, where the source, lens, and observer are colinear, no such plan is defined. A light ray which passes the lens at a distance ξ is deflected by $\hat{\alpha}$, given by (3.1). The condition that this ray reaches the observer is obtained solely from the geometry of Figure 1, namely

$$\beta D_s = \frac{D_s}{D_d} \xi - \frac{2R_s}{\varepsilon} D_{ds} \quad (3.3)$$

Here, D_{ds} is the distance of the source from the lens. In the simple case with a Euclidean background metric considered here, $D_{ds} = D_s - D_d$; however, since gravitational lensing occurs in the universe on large scales (among the hitherto detected GL events, most of the sources are QSOs with redshift typically larger than 1), one must use a cosmological model. There, distance does not have an unambiguous meaning, but several distances can be defined in analogy with Euclidean laws. The distances in (3.3) must then be interpreted as angular-diameter distances, empty cone angular diameter distances for which in general, $D_{ds} \neq D_s - D_d$. Denoting the angular separation between the deflecting mass and the deflected ray by

$$\theta = \frac{\xi}{D_d} \quad (3.4)$$

we obtain from (3.3) the lens equation,

$$\beta = \theta - \frac{2R_s D_{ds}}{D_d D_s} \frac{1}{\theta} \quad (3.5)$$

we allow β and θ to have either sign. This expression clearly shows that the problem under consideration involves a characteristic angle α_0 and a characteristic length, ξ_0 , in the lens plane, given by

$$\alpha_0 = \sqrt{2R_s \left(\frac{D_{ds}}{D_d D_s} \right)} \quad (3.6)$$

$$\xi_0 = \sqrt{2R_s \frac{D_d D_{ds}}{D_s}} = \sqrt{\left(\frac{4GM}{c^2} \right) \left(\frac{D_d D_{ds}}{D_s} \right)} = \alpha_0 D_d \quad (3.7)$$

In addition, there is a characteristic length scale in the source plane, given by

$$\eta_0 = \sqrt{2R_s \frac{D_s D_{ds}}{D_d}} = \sqrt{\left(\frac{4GM}{c^2}\right) \left(\frac{D_s D_{ds}}{D_d}\right)} = \alpha_0 D_s \quad (3.8)$$

The interpretation of these quantities will soon become clear. Writing (3.5) as

$$\beta = \theta - \frac{\alpha_0^2}{\theta}$$

or

$$\theta^2 - \beta\theta - \alpha_0^2 = 0 \quad (3.9)$$

We obtain

$$\theta_{1,2} = \frac{1}{2}(\beta \pm \sqrt{4\alpha_0^2 + \beta^2}) \quad (3.10)$$

The angular separation between the images (lens) is

$$\Delta\theta = \theta_1 - \theta_2 = \sqrt{4\alpha_0^2 + \beta^2} \geq 2\alpha_0 \quad (3.11)$$

and the true angular separation between the source and the deflector is related to the image positions by

$$\theta_1 + \theta_2 = \beta \quad (3.12)$$

Thus, the ray-trace equation always has two solutions of opposite sign. This means that the source has an image on each side of the lens. We show below that the two images are of comparable brightness only if β , and hence $|\theta|$, is of order α_0 . Therefore, the typical angular separation of the two images is close to its minimum $2\alpha_0$, and the corresponding typical impact parameter is ξ_0 .

Typical length and angular scales. In practice, two cases of lensing situations are of importance. First, if both lens and source are at cosmological distances, the factors $\frac{D_d D_{ds}}{D_s}$ and $\frac{D_d D_s}{D_{ds}}$ will be fair fractions η and η_1 , respectively, of the Hubble length c/H_0 :

$$\frac{D_d D_{ds}}{D_s} = \eta \frac{c}{H_0}, \quad (3.13)$$

$$\frac{D_d D_s}{D_{ds}} = \eta_1 \frac{c}{H_0}, \quad (3.14)$$

where H_0 is the Hubble constant. Measuring H_0 in units of $50 \text{ km s}^{-1} \text{ Mpc}^{-1}$, $H_0 = h_{50} \cdot (50) \text{ km s}^{-1} \text{ Mpc}^{-1}$, the Hubble length is

$$\frac{c}{H_0} \approx h_{50}^{-1} (1.8 \times 10^{28}) \text{ cm} \approx 5.8 \times 10^9 h_{50}^{-1} \text{ pc} \quad (3.15)$$

The angular scale α_0 is then

$$\alpha_0 \approx 1.2 \times 10^{-6} \sqrt{\frac{M}{M_\odot}} \sqrt{\frac{h_{50}}{\dot{\eta}}} \text{ arcsec}, \quad (3.16)$$

where $M_\odot = 1.989 \times 10^{33} \text{ g}$ is the Sun's mass, and $\frac{4GM_\odot}{c^2} = 2R_{s\odot} \approx 5.9 \text{ km}$. The corresponding length scale is

$$\varepsilon_0 \approx 10^{17} \sqrt{\frac{M}{M_\odot}} \sqrt{\frac{\eta}{h_{50}}} \text{ cm} \approx 0.03 \sqrt{\frac{M}{M_\odot}} \sqrt{\frac{\eta}{h_{50}}} \text{ pc} \quad . \quad (3.17)$$

The second case that is frequently discussed is $D_d \ll D_{ds} \approx D_s$; then

$$\alpha_0 \approx 3 \times 10^{-3} \sqrt{\frac{M}{M_\odot}} \left(\frac{D_d}{1 \text{ kpc}}\right)^{-1/2} \text{ arcsec} \quad (3.18)$$

and

$$\xi_0 \approx 4 \times 10^{13} \sqrt{\frac{M}{M_\odot}} \left(\frac{D_d}{1 \text{ kpc}}\right)^{-1/2} \text{ cm} \quad (3.19)$$

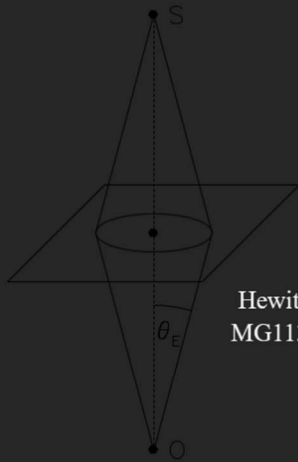
For the nearest observed gravitational lens system, the lens is a spiral galaxy at redshift $D_d = 0.039$; if we take $M = 10^{12} \text{ Mev}$, we get $\xi_0 = 7 h_{50}^{-\frac{1}{2}} \text{ kpc}$. As mentioned above, the images are of comparable brightness only if β is sufficiently small that $|\theta| = \alpha_0$. This means that, with respect to lensing, any spherically symmetric matter distribution can be treated as a point mass if its radius is less than, say, $\frac{\xi_0}{3}$, since the exterior of a spherically symmetric mass distribution is always described by the Schwarzschild metric.

Einstein rings. A special situation arises if source, lens and observer are colinear, i.e., $\beta = 0$. In this case, there is no preferred plane for the light rays to propagate, but the whole configuration is rotationally symmetric about the line-of-sight to the lens. For $\beta = 0$, the solutions (3.10) become $\theta_{1,2} = \pm\alpha_0$; hence, due to symmetry, the whole ring of angular radius $\theta = \alpha_0$ is a solution to the lens equation. A point source exactly behind the lens would thus appear, according to ray optics, as a circle around the lens. However, in this idealized case, infinitely many light rays with exactly equal path length intersect at the observer, and therefore diffraction and interference invalidate geometrical optics. In contrast, any real source is extended and not strictly monochromatic. Then, (i) those parts of a wave train emitted from a source point S located not on, but near the axis OM, which reaches the observer from directions corresponding to the two geometrical images of S, arrive there separated in time, if the time delay exceeds the coherence time; and (ii) waves from different source points are incoherent. Therefore, unresolved, extended sources, nearly aligned with deflector and observer, produce nearly the same ring images which geometrical optics predicts for the idealized case. Ring-shaped images of point sources can only occur in lensing situations with axially symmetric matter distributions; they arise solely from symmetry. On the other hand, extended sources can have ring-shaped images even if the lens is not perfectly symmetric. Such images are frequently called Einstein ring.

Einstein Ring

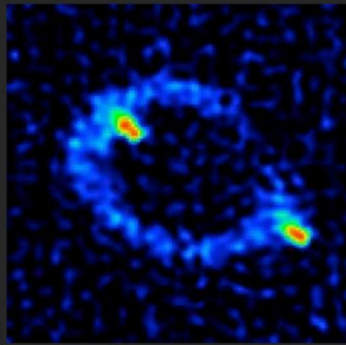
When lens, source, and observer lie on the same line get Einstein ring

$$\theta_E = \sqrt{\frac{4GM}{c^2} \frac{D_{LS}}{D_s D_L}}$$

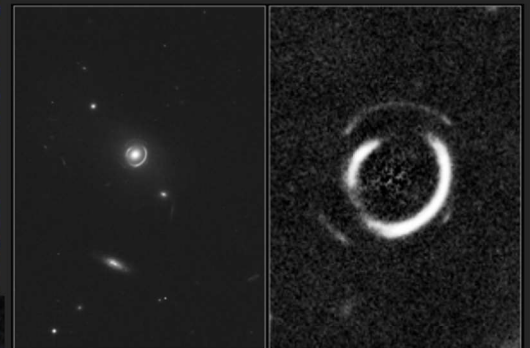


Hewitt+ 1987
MG1131+0456

SDSSJ1430



Double Einstein Ring - v. rare



Gavassi+ 2008

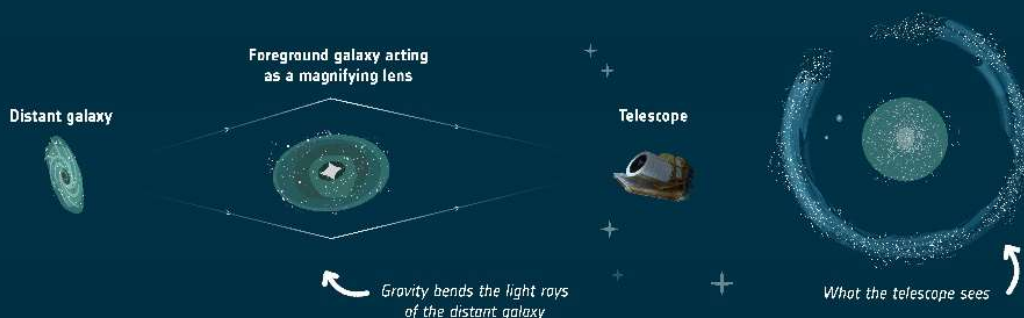
Einstein radius depends on lens mass
AND geometry



A. Bolton (UH IIA) for SLACS and NASA/ESA

EINSTEIN RING – EXPLAINED

When we observe a distant galaxy with our telescope, its light may encounter another galaxy on its way to us. The foreground galaxy acts like a magnifying lens, bending the travelling light rays due to its gravity. This is called gravitational lensing. If the background galaxy, the lensing galaxy, and the telescope are perfectly aligned, the image appears as a ring – called an Einstein ring.



Several authors discussed G.L. as evidence to explain different astrophysics problem such as the dark matter & dark energy, massive objects, quasars and galaxies cluster and so on. Here we will discuss short notes about some of these models.

3.2.3 Theoretical description of some models

1- The gravitational lensing due to Schwarzschild black hole

The Schwarzschild metric describes the simplest type of black hole-a non-rotating, uncharged black hole, known as a Schwarzschild black hole. It was derived by Schwarzschild in 1916, shortly after Einstein proposed his theory of General Relativity. The Schwarzschild metric is a solution to Einstein's field equations in a vacuum, meaning there is no matter present except for a central singularity. The key characteristic of this metric is that it describes spherically symmetric gravitational fields. The Schwarzschild metric remains a foundational solution for understanding black hole physics in general relativity. A Schwarzschild black hole can form when a massive star collapses under its own gravity. If the core's mass is greater than a limit which is known as Tolman Oppenheimer-Volkoff limit, no force can counterbalance the gravitational collapse, leading to the formation of a black hole. The gravitational lensing occurs when the gravity of a bigger objects such as galaxy or a cluster of galaxies, bends the light from a more distant object, like another galaxy or a quasar, as it travels toward an observer. This phenomenon can distort, magnify, or even create multiple images of the background object. There are several key uses and applications of gravitational lensing in astrophysics and cosmology. Despite past and ongoing research done on gravitational lensing, it has not been able to answer many questions in astrophysics yet, one of them is the nature of dark matter. Gravitational lensing is a powerful tool for both observational astronomy and theoretical astrophysics, offering insight into the structure, composition, and evolution of the universe. Moreover, gravitational lensing has been used to probe dark matter and dark energy, measuring the mass of cosmic structures, probing the early Universe, detecting exoplanets, Hubble constant measurement and, discovering hidden objects. Hence gravitational lensing is crucial in astrophysics. The motivation to do the current work is to simulate the black holes with different galaxies that were kept in the background to find the gravitational lensing.

2- Self-lensing of a singular isothermal sphere (SIS) model

The singular isothermal sphere (SIS) density profile is the simplest parameterization of the spatial distribution of matter in an astronomical system (e.g. galaxies, clusters of galaxies and so on. Many astrophysical systems can be approximated as isothermal spheres, an isothermal sphere, such as globular clusters, elliptical galaxies, clusters of galaxies. They usually consist of smaller particles which are more compact objects, like stars or galaxies. In an isothermal sphere, the foreground object can act as lenses on background objects in the same distribution from the outside, i.e. in projection, light from the background particle has to pass near the foreground particle, and hence it is affected by their gravitational attraction [3].

This effect of self-lensing by a stellar disk. Self-lensing by an isothermal sphere is a simple, well-defined problem which may have interesting applications.

The singular isothermal sphere (SIS) density equation is described by

$$\rho(r) = \frac{\sigma_v^2}{2\pi G r^2}$$

where σ_v^2 is the one-dimensional velocity dispersion and G is Newton's constant.

The SIS profile is unphysical because of the singularity at zero radius and the fact that the total mass calculated by integrating the function out to infinite radius does not converge (is infinite).

3-The Navarro-Frenk-White (NFW) profile model

The Navarro–Frenk–White (NFW) profile is a spatial mass distribution of dark matter fitted to dark matter halos identified in N-body [4,8]. The NFW profile is one of the most used model profiles for dark matter halos. The substantial impact of NFW's work on theoretical understanding of cosmic structure formation can be traced to three key insights.

1) In cosmological models where dark matter structure grows hierarchically from weak initial fluctuations, dark matter halos are almost self-similar; halo regions which are close to dynamical equilibrium are adequately represented for all masses, and at all times by a simple analytic formula with only two free parameters, a characteristic density and a characteristic size.

2) These two parameters are related with rather little scatter; larger halos are less dense. The size density relation depends on cosmological parameters and so can be used to constrain these observationally.

3) The characteristic density of a halo is linked to the mean density of the universe at its epoch of maximal growth. Thus, the size-density relation reflects the fact that larger halos typically assembled at later times.

They suggest a density that decreases with distance from the center. The NFW density profile of dark matter as a function of radius is given by:

$$\rho(r) = \frac{\rho_0}{\frac{r}{R_s} \left(1 + \frac{r}{R_s}\right)^2}$$

where R_s is the scale radius parameters which vary from halo to halo and ρ_0 is characteristic density. Also, the integrated mass within some radius R_{\max} is given by

$$M = \int_0^{R_{\max}} 4\pi r^2 \rho(r) dr = 4\pi \rho_0 R_s^3 \left[\ln\left(\frac{R_s + R_{\max}}{R_s}\right) - \frac{R_{\max}}{R_s + R_{\max}} \right].$$

The total mass is divergent, but it is often useful to take the edge of the halo to be the virial radius, R_{vir} , which is related to the concentration parameter (c) and scale radius via $R_{\text{vir}} = cR_s$. The total mass in halo within R_{vir} is described by

$$M = \int_0^{R_{\text{vir}}} 4\pi r^2 \rho(r) dr = 4\pi \rho_0 R_s^3 \left[\ln(1 + c) - \frac{c}{1 + c} \right].$$

Thus, the specific value of c is roughly 10 or 15 for the Milky Way and may range from 4 to 40 for halos of various sizes. Also, the mean density of a dark matter halo is given by

$$\rho(r) = \frac{\rho_{\text{halo}}}{3A_{\text{NFW}} x(c^{-1} + x)^2}$$

where

$$\rho_{\text{halo}} \equiv M / \left(\frac{4}{3} \pi R_{\text{vir}}^3 \right), \text{ is the mean density of the halo,}$$

$$A_{\text{NFW}} = \left[\ln(1 + c) - \frac{c}{1 + c} \right], \text{ is from the mass calculation, and}$$

$$x = r/R_{\text{vir}} \text{ is the fractional distance to the virial radius.}$$

In addition, the integral of the squared density is

$$\int_0^{R_{\max}} 4\pi r^2 \rho(r)^2 dr = \frac{4\pi}{3} R_s^3 \rho_0^2 \left[1 - \frac{R_s^3}{(R_s + R_{\max})^3} \right]$$

so that the mean squared density inside of R_{\max} is

$$\langle \rho^2 \rangle_{R_{\max}} = \frac{R_s^3 \rho_0^2}{R_{\max}^3} \left[1 - \frac{R_s^3}{(R_s + R_{\max})^3} \right],$$

which for the virial radius simplifies to become

$$\langle \rho^2 \rangle_{R_{\text{vir}}} = \frac{\rho_0^2}{c^3} \left[1 - \frac{1}{(1+c)^3} \right] \approx \frac{\rho_0^2}{c^3}$$

and the mean squared density inside the scale radius is simply described by

$$\langle \rho^2 \rangle_{R_s} = \frac{7}{8} \rho_0^2$$

Also, by solving Poisson's equation, gravitational potential becomes

$$\Phi(r) = -\frac{4\pi\rho_0 R_s^2}{r} \ln\left(1 + \frac{r}{R_s}\right).$$

With the limits $\lim_{r \rightarrow \infty} \Phi = 0$ and $\lim_{r \rightarrow 0} \Phi = -4\pi\rho_0 R_s^2$.

Therefore, the acceleration due to the NFW potential can be written in the form

$$a = -\nabla \Phi_{\text{NFW}}(r) = G \frac{M_{\text{vir}}}{\ln(1+c) - c/(1+c)} \frac{\frac{r}{r+R_s} - \ln\left(1 + \frac{r}{R_s}\right)}{r^3} r$$

Where r is the position vector and $M_{\text{vir}} = \frac{4\pi}{3} r_{\text{vir}}^3 200\rho_{\text{crit}}$. Meanwhile, the radius of the maximum circular velocity (R_{\max}) can be found from the maximum of $M(r)/r$ as $R_{\text{Crit}}^{\text{Max}} = \alpha R_s$. Where $\alpha = 2.16258$ is the positive root of: $\ln(1+\alpha) = \frac{\alpha(1+2\alpha)}{(1+\alpha)^2}$, maximum circular velocity is also related to the characteristic density and length scale of NFW profile become

$$V_{\text{circ}}^{\text{max}} \approx 1.64 R_s \sqrt{G\rho_0}$$

Furthermore, over a broad range of halo mass and redshift, the NFW profile approximates the equilibrium configuration of dark matter halos produced in simulations of collisionless dark matter particles. Simulations assuming different cosmological initial conditions produce halo populations in which the two parameters of the NFW profile follow different mass-

concentration relations, depending on cosmological properties such as the density of the universe and the nature of the very early process which created all structures.

4- Gravitational lensing effect in traversable wormholes

The effect of strong gravitational lensing in the context of charged wormhole. The conditions determining the existence of photon spheres at and outside the throat are obtained. Furthermore, photon spheres are investigated in three cases for three different forms of redshift function. These three cases include the existence of effective photon spheres (i) at the throat, (ii) outside the throat and (iii) both at and outside the throat. Consequently, these provide information about the formation of infinite numbers of concentric rings and may lead to the detection of wormhole geometries. This paper explains the effect of gravitational lensing on charged wormholes by deriving the necessary and sufficient conditions for the existence of photon spheres at or outside the throat of the charged wormhole. Furthermore, the existence of photon spheres is examined for three different and novel forms of redshift function and the formation of infinite number of concentric rings is obtained [5].

3.2.4 Observations

Although identifying gravitational lensing (GL) systems may seem straightforward, it presents significant challenges [1]. Quasars (QSOs) and distant galaxies are prime candidates for GL searches due to their distance from Earth. QSOs are advantageous because of their high luminosity, simple optical structure, and strong emission lines, but their stellar appearance, faintness due to high redshifts, and low sky density make them difficult to identify without spectroscopy. Despite these drawbacks, QSOs led early GL discoveries, as the first confirmed lensing systems involved QSOs lensed by intervening galaxies. Distant galaxies, while fainter and more complex due to weak or broken spectral lines, have a much higher population density than QSOs. Recently, several GL systems involving galaxies have been found, mainly because of the dramatic distortions caused by massive intervening galaxy clusters. The study of GL systems is divided into those involving point sources (QSOs) and extended sources (galaxies), each with distinct detection and confirmation methods, as well as observational challenges. While theory predicts that a non-singular mass lens produces an odd number of images, observational effects like demagnification often obscure the faintest images, resulting in even-numbered configurations. The simplest observed systems show two images, progressing up to four. Beyond this, the field expands into the study of arcs and rings (features of extended sources) which is now a rapidly growing and increasingly prominent area in GL research.

Eddington and the Eclipse

Using data taken during a solar eclipse in 1919, Eddington measured a value close to that of the GR prediction

DETERMINATION OF DEFLECTION OF LIGHT BY THE SUN'S GRAVITATIONAL FIELD. 331

Dyson, Eddington,
& Davidson 1920

The result from declinations is about twice the weight of that from right ascensions, so that the mean result is

$$1''.98$$

with a probable error of about $\pm 0''.12$.

The Principe observations were generally interfered with by cloud. The unfavourable circumstances were perhaps partly compensated by the advantage of the extremely uniform temperature of the island. The deflection obtained was

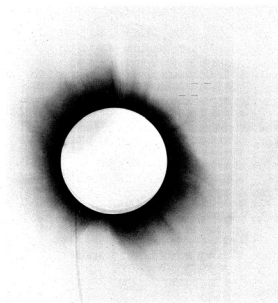
$$1''.61.$$

The probable error is about $\pm 0''.30$, so that the result has much less weight than the preceding.

Both of these point to the full deflection $1''.75$ of EINSTEIN'S generalised relativity theory, the Sobral results definitely, and the Principe results perhaps with some uncertainty. There remain the Sobral astrographic plates which gave the deflection

$$0''.93$$

discordant by an amount much beyond the limits of its accidental error. For the reasons already described at length not much weight is attached to this determination.



332 SIR F. W. DYSON, PROF. A. S. EDDINGTON AND MR. C. DAVIDSON ON A

Thus the results of the expeditions to Sobral and Principe can leave little doubt that a deflection of light takes place in the neighbourhood of the sun and that it is of the amount demanded by EINSTEIN'S generalised theory of relativity, as attributable to the sun's gravitational field. But the observation is of such interest that it will

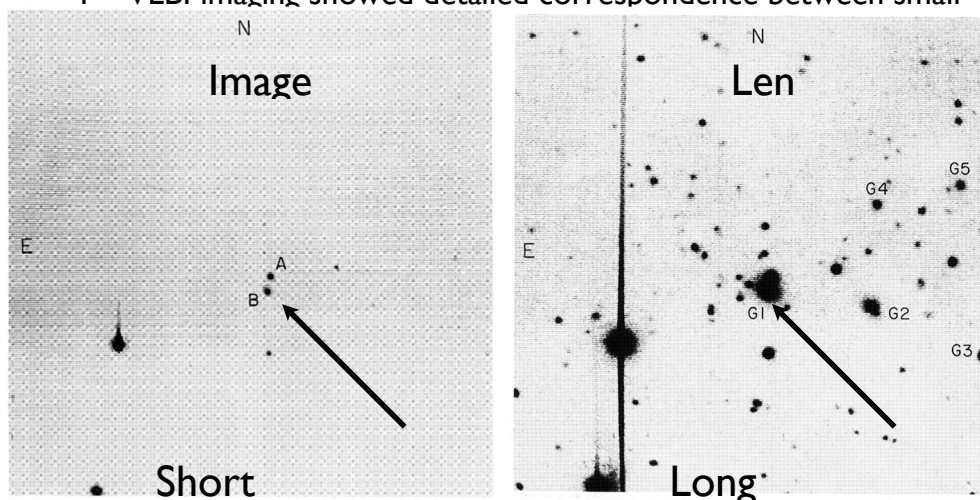
(bizzarely if not
for this then
Eddington might
well have been
imprisoned for
being a pacifist)

The first gravitational lens (GL) candidate was discovered in 1979 by Walsh, Carswell, and Weymann (0957+561), marking the beginning of a rapidly growing list of candidates. While some of these have since been confirmed as true GL systems, others remain ambiguous, especially when the lensing galaxy cannot be identified. The first confirmed GL, 0957+561, was found during a survey of radio sources at 966 MHz at Jodrell Bank, aiming to identify optical counterparts. Among these, a pair of blue stellar objects (A and B) separated by 6 arcseconds, were discovered. Though overlapping on the Palomar Observatory Sky Survey, they were distinguishable and of similar brightness, making their identification as counterparts tentative due to an offset of 17 arcseconds from the radio source's position. Spectroscopic analysis revealed nearly identical spectra with redshifts of 1.405, suggesting they were not separate QSOs but lensed images of the same QSO. The difference in color (B appearing redder) was attributed to differential reddening, implying the presence of a lensing

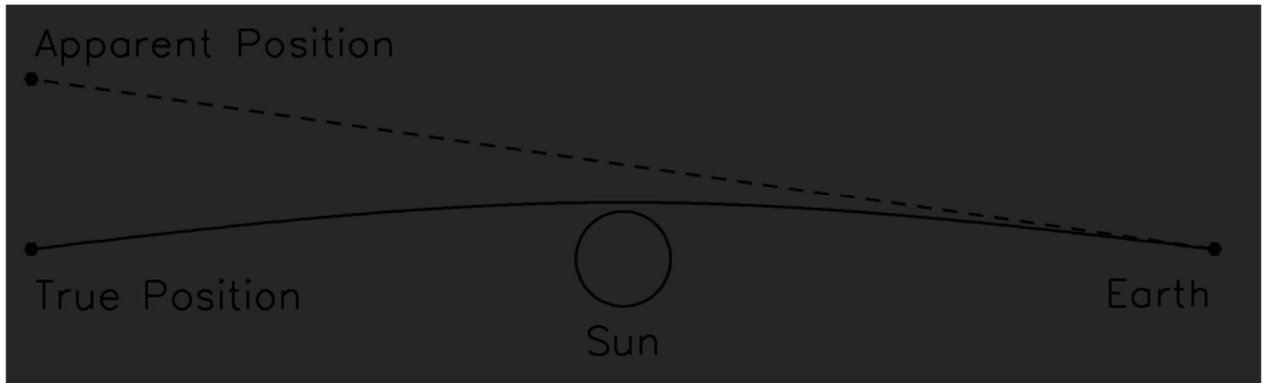
galaxy closer to image B. Indeed, a galaxy named G1 was detected just north of B, fitting a King profile with a core radius of ~ 0.24 arcseconds and an ellipticity of 0.13. Thus, G1 was later found to be the brightest galaxy in a cluster, with its redshift refined to 0.36. It did not lie directly between A and B, indicating the lens is not a symmetric mass distribution. Early radio observations using the Very Large Array (VLA), which became operational shortly after the QSO's identification, revealed a complex radio structure with four components, two matching optical images. These findings, along with the minimal redshift differences (both absorption and emission), supported the GL hypothesis. The estimated magnification of image A was about four times, and the lens mass was approximated as proportional to the redshift times 10^{13} solar masses. This discovery not only marked the first clear case of gravitational lensing but also highlighted both the promise and complexity of identifying and interpreting such systems.

Discovery of

- The first concrete example of a gravitational lens was reported in the form of the quasar QSO 957+561 A,B found (Walsh, Carswell & Weymann 1979). Two seen images
- Evidence that this is a lens comes
 - 1 Lensing galaxy detected at
 - 2 Similarity of the spectra of the two
 - 3 Ratio of optical and radio fluxes are consistent between
 - 4 VLBI imaging showed detailed correspondence between small



Einstein's prediction was famously confirmed in 1919 by Eddington's solar eclipse expedition, which observed the deflection of starlight around the Sun. This landmark observation provided crucial evidence supporting general relativity and sparked interest in the phenomenon of gravitational lensing.



3.2.4.1 Photometry in Astronomy

Photometry is a fundamental technique in astronomy concerned with measuring the flux or intensity of light radiated by celestial objects [11]. This measurement, typically performed using a telescope equipped with a photometer (often a CCD or photoelectric device), allows astronomers to quantify the brightness or apparent magnitude of stars, galaxies, and other cosmic sources. By calibrating these measurements against standard stars with known intensities and colors, precise and reliable data on the luminous properties of astronomical objects can be obtained.

The process of photometry involves gathering light from a celestial object and often passing it through specialized photometric optical bandpass filters. These filters isolate specific ranges of wavelengths, allowing for the study of an object's brightness in different colors. Standardized sets of these passbands, known as photometric systems, are crucial for ensuring accurate comparison of observations across different telescopes and studies [11]. While basic photometry measures the total light within a given bandpass, a more advanced technique called spectrophotometry utilizes a spectrophotometer to observe both the amount of radiation and its detailed spectral distribution [12].

The Role of Photometry in Studying Gravitational Lensing

Since gravitational lensing occurs when the gravitational field of a massive object (such as a galaxy or a cluster of galaxies) bends the light from a more distant source. This bending can result in multiple images of the background source, magnification of its brightness, and

distortion of its shape [1]. Consequently, photometry plays a crucial role in understanding and analyzing these lensing effects in several keyways

Astronomers can quantify the magnification caused by the gravitational lens by measuring the brightness of the lensed images compared to the expected brightness of the un-lensed source (if it could be observed directly). Photometry in different band passes can reveal wavelength-dependent magnification effects, providing insights into the mass distribution of the lensing object and the properties of the source.

In addition, gravitational lensing can produce multiple images of the same background object. Photometric measurements can confirm that these separate images originate from the same source by comparing their colors and brightness variations over time. Similar photometric properties across multiple images strengthen the case for common origin and lensing.

To study source properties: The magnification caused by lensing can make faint and distant objects bright enough to study their photometric properties in detail. This allows astronomers to investigate the colors, stellar populations, and even variability of galaxies that would otherwise be too faint to observe.

Also, to map mass distributions of lenses: By analyzing the distortions and magnifications of many background sources lensed by a foreground object, and by using precise photometry to quantify these effects, astronomers can create detailed maps of the mass distribution (including dark matter) within the lensing galaxy or cluster.

Moreover, Photometry is the primary tool for detecting microlensing events, where a compact object (like a star or a black hole) passes in front of a more distant star, causing a temporary increase in the background star's brightness. The shape and duration of these photometric light curves provide information about the mass and relative motion of the lensing object [12].

3.2.4.2 Observation evidence of dark matter and energy

To explain and observe dark matter and energy, there exist different methods and analysis, such as: Galaxy rotation curves, Velocity dispersion and Galaxy clusters.

Galaxy clusters are particularly important for dark matter studies since their masses can be estimated in three independent ways:

- i) From the scatter in radial velocities of the galaxies within clusters.
- ii) From X-rays emitted by hot gas in the clusters. From the X-ray energy spectrum and flux, the gas temperature and density can be estimated, hence giving the pressure; assuming pressure and gravity balance determines the cluster's mass profile.

Iii) Gravitational lensing (usually of more distant galaxies) can measure cluster masses without relying on observations of dynamics (e.g. velocity).

Gravitational lensing

One of the consequences of general relativity is gravitational lens. Gravitational lensing occurs when massive objects between a source of light and the observer act as a lens to bend light from this source. Also, lensing does not depend on the properties of the mass; it only requires there to be a mass. The more massive an object, the more lensing is observed. An example is a cluster of galaxies lying between a more distant source such as a quasar and an observer. In this case, the galaxy cluster will lens the quasar. Furthermore, Strong lensing is the observed distortion of background galaxies into arcs when their light passes through such a gravitational lens. It has been observed around many distant clusters including Abell 1689 [13]. By measuring the distortion geometry, the mass of the intervening cluster can be obtained. In the weak regime, lensing does not distort background galaxies into arcs, causing minute distortions instead. By examining the apparent shear deformation of the adjacent background galaxies, the mean distribution of dark matter can be characterized. The measured mass-to-light ratios correspond to dark matter densities predicted by other large-scale structure measurements.

Dark matter is detected through its gravitational interactions with ordinary matter and radiation. As such, it is very difficult to determine what the constituents of cold dark matter are. The candidates fall roughly into three categories:

Axions, very light particles with a specific type of self-interaction that makes them a suitable CDM candidate.

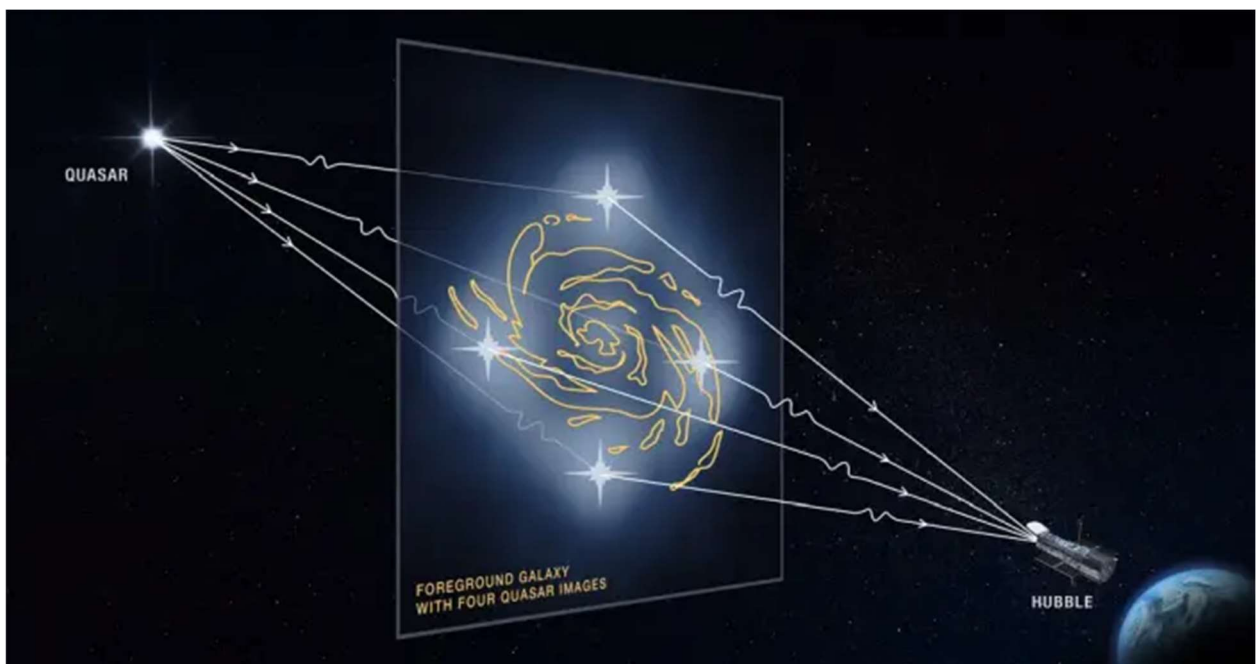
Weakly interacting massive particles (WIMPs). There is no currently known particle with the required properties, but many extensions of the standard model of particle physics predict such particles. Massive compact halo objects (MACHOs), large, condensed objects such as black holes, neutron stars, white dwarfs, very faint stars, or non-luminous objects like planets. The search for these objects consists of using gravitational lensing to detect the effects of these objects on background galaxies. Most experts believe that the constraints from those searches rule out MACHOs as a viable dark matter candidate.

Examples of Strong, Weak and Micro lensing

1- Strong Lensing Example: Einstein Cross

One of the most famous examples of strong gravitational lensing is the Einstein Cross (Q2237+030 or G2237+0305). In this system, a quasar located about 8 billion light-years away is lensed by a foreground galaxy approximately 400 million light-years away. The gravitational field of the galaxy bends the light from the quasar, forming four distinct images arranged around the galaxy's core. This dramatic example of strong lensing has been essential for studying quasar variability and testing general [14].

1-Strong lensing



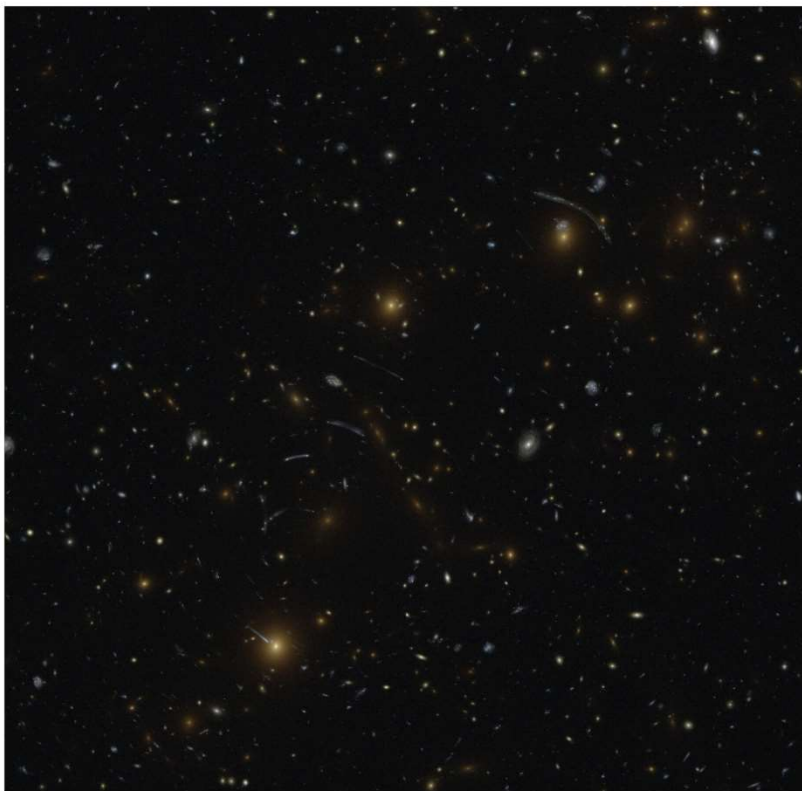
Ref. [15]

Another well-known strong lensing system is the **Abell 1689 galaxy cluster**, which produces spectacular arcs and multiple images of background galaxies due to its immense gravitational potential. The cluster's strong lensing effect has enabled astronomers to map its dark matter distribution in unprecedented detail [14].



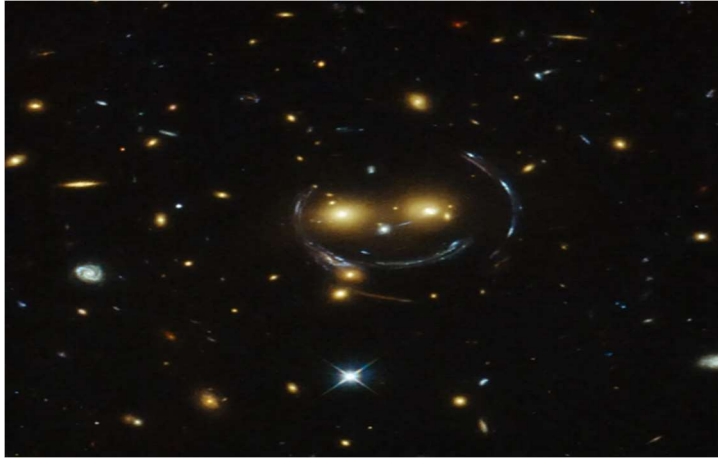
Ref. [15]

2- Weak Lensing Example: Cosmic Shear in the Hubble Space Telescope Surveys



Ref. [15]

Weak lensing effects are observed on much larger scales and are often used to map the dark matter distribution in the universe. One of the most significant discoveries from weak gravitational lensing comes from the **Hubble Space Telescope Cosmic Evolution Survey (COSMOS)**. This survey analyzed subtle distortions in galaxy shapes caused by the large-scale structure of the universe.



Ref. [16]

The **Canada-France-Hawaii Telescope Lensing Survey (CFHTLenS)** also provided groundbreaking weak lensing results by mapping dark matter across vast cosmic distances. By measuring tiny statistical distortions in background galaxy shapes, astronomers were able to reconstruct the dark matter distribution and refine models of cosmic structure formation.

These examples highlight how both strong and weak lensing serve as powerful tools for exploring the universe's hidden structure and deepening our understanding of gravity's role in shaping the cosmos [17,18].

3-Micro lensing [19].

Microlensing

Einstein radius for a solar mass lens in the galaxy and a source located in the LMC

$$\theta_E = (0.9 \text{ mas}) \left(\frac{M}{M_\odot} \right)^{1/2} \left(\frac{D}{10 \text{ kpc}} \right)^{-1/2}$$

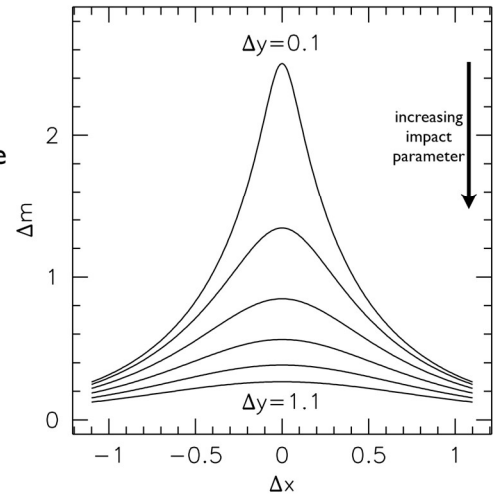
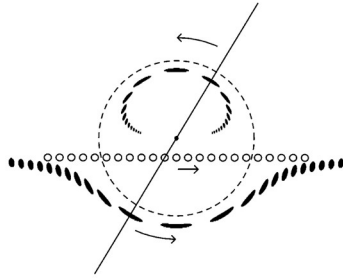
Too small to resolve individual images with optical telescope, but can see the effect of magnification

For sources that pass inside the lens Einstein radius

$$\mu \geq 1.34 \longrightarrow \text{mag} \geq 0.32$$

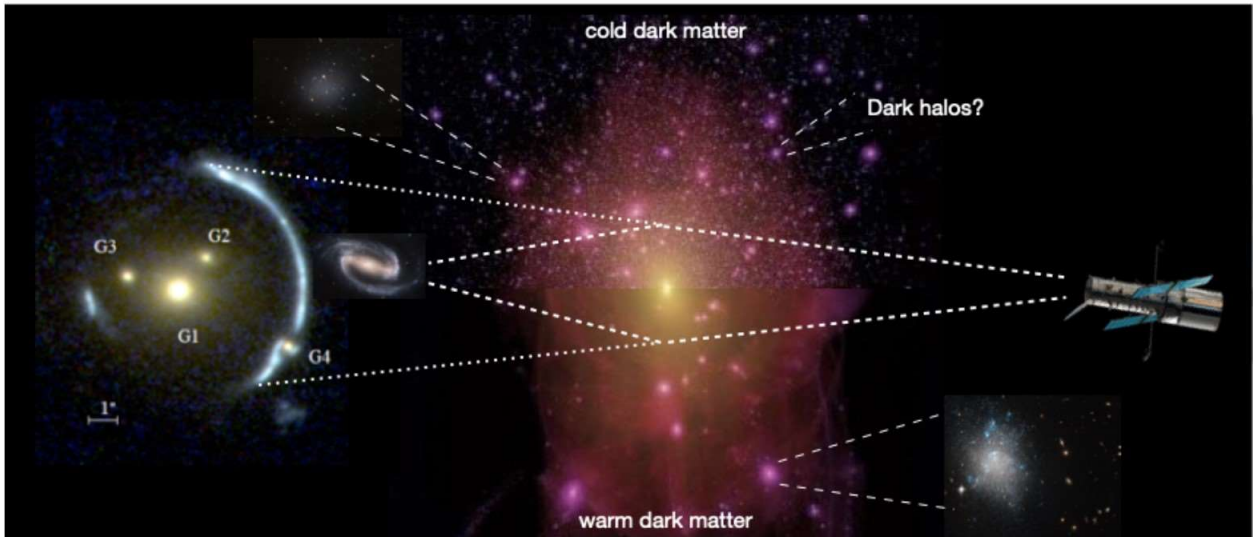
Readily observable change in source magnitude

Light curve gives impact parameter and time scale

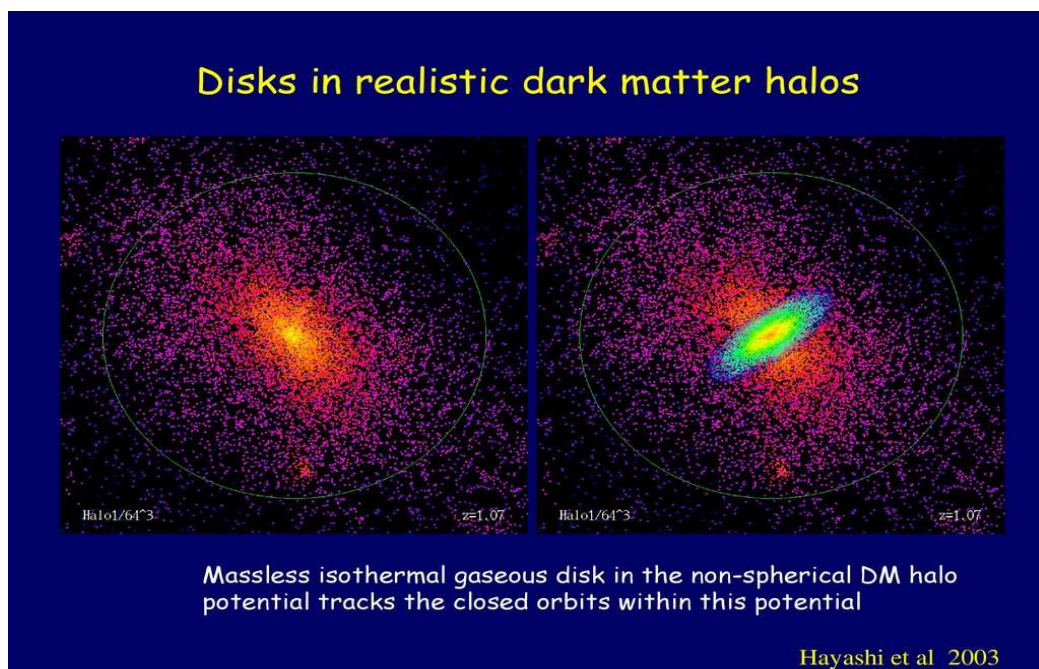


Afterward, halo observations:

The dark matter density profiles of massive galaxy clusters can be measured directly by gravitational lensing and agree well with the NFW profiles predicted for cosmologies with the parameters inferred from other data. For lower mass halos, gravitational lensing is too noisy to give useful results for individual objects, but accurate measurements can still be made by averaging the profiles of many similar systems. For the main body of the halos, the agreement with the predictions remains good down to halo masses as small as those of the halos surrounding isolated galaxies like our own. The inner regions of halos are beyond the reach of lensing measurements, however, and other techniques give results which disagree with NFW predictions for the dark matter distribution inside the visible galaxies which lie at halo centers [20].



Ref. [20]



Ref. [20]

Chapter 4: Discussion

4.1 Conclusion

In this project, we gave a brief understanding of the phenomena of gravitational lensing, which all comes down to Einstein's general theory of relativity. and how gravity from massive objects can bend light from even farther away. We looked at this idea, the different ways to think about it in both Newtonian and the more accurate relativistic way, and some of the theoretical models that help explain it.

Moreover, gravitational lensing not only validates general relativity but also serves as a powerful, model-independent probe of mass distributions in the universe. From the comparative analysis of the NFW and SIS profiles reveals that the inner density slope and core structure critically shape observable lensing effects, for instance, the SIS model produces relatively simple, symmetric two-image systems, while the NFW model produces center and extended halo generate more complex magnification patterns and multiple images. These findings emphasize the necessity of selecting an appropriate mass model when reconstructing lensing masses from observational data. Looking ahead, integrating lensing analyses with complementary techniques, such as stellar dynamics and X-ray mapping, will give more precise characterizations of dark-matter halos and advance our understanding of cosmic structure formation.

4.2 Reference

- [1] Schneider, P. Ehlers, J. and Falco, E. E. (1992). Gravitational lenses. 2nd printing 1999, Astro. and APh. library, springer.
- [2] Narayan, R. and Bartelmann, M. (1996). Lectures on gravitational lensing. arXiv:astro-ph/9606001.
- [3] Kormann, R. Schneider, P. and Bartelmann, M. (1994). Isothermal elliptical gravitational lens models. Astronomy and Astrophysics, 284, 285–299.
- [4] Navarro, J. F. Frenk, C. S. and White, S. D. M. (1996). the structure of cold dark matter halos. Astrophysical Journal, 462, 563.
- [5] Godani, N. and Samanta, G. C. (2021). *Gravitational lensing effect in traversable wormholes*. arXiv:2105.08517v1.
- [6] Gao, X. J. Chen, J. M. Zhang, H. Yin, Y. and Hu, Y.P. (2021). *Investigating strong gravitational lensing with black hole metrics modified with an additional term*. Physics Letters B, 822, 136683.
- [7] Del Popolo, A. and Giani, L. (2022). *Constraining scalar field models using strong gravitational lensing*. The European Physical Journal C, 82, 419.
- [8] Mehrotra, A. and Kanishka, R. (2024). *The gravitational lensing due to Schwarzschild black holes*. arXiv:2409.20452v1.
- [9] Heyrovský, D. and Karamazov, M. (2024). *Gravitational lensing by an ellipsoidal Navarro–Frenk–White dark-matter halo*. arXiv:2404.00169v2.
- [10] Bartelmann, M. (2010). Gravitational lensing. Classical and Quantum Gravity, 27(23), 233001.
- [11] Photometry (optics) [https://en.wikipedia.org/wiki/Photometry_\(optics\)](https://en.wikipedia.org/wiki/Photometry_(optics))
- [12] Photometry (astronomy) [https://en.wikipedia.org/wiki/Photometry_\(astronomy\)](https://en.wikipedia.org/wiki/Photometry_(astronomy))
- [13] NASA Image – Galaxy Cluster Abell 1689
<https://science.nasa.gov/image-detail/galaxy-cluster-abell-1689-3/>
- [14] Treu, T. (2010). Strong lensing by galaxies. Annual Review of Astronomy and Astrophysics, 48(1), 87–125.

- [15] NASA Asset – The Gravitational Lens G2237+0305
<https://science.nasa.gov/asset/hubble/the-gravitational-lens-g2237-0305/>
<https://www.constellation-guide.com/einstein-cross/>
- [16] NASA Hubble – Science Behind Gravitational Lenses
<https://science.nasa.gov/mission/hubble/science/science-behind-the-discoveries/hubble-gravitational-lenses/>
- [17] Mandelbaum, R. (2018). Weak gravitational lensing for precision cosmology. Annual Review of Astronomy and Astrophysics, 56, 393–433.
- [18] A. Refregier, A. (2003). weak gravitational lensing by large-scale structure. Annual Review of Astronomy and Astrophysics, vol. 41
- [19] Gravitational microlensing https://en.wikipedia.org/wiki/Gravitational_microlensing
- [20] <https://kipac.stanford.edu/highlights/between-worlds-visible-and-invisible-lies-dark-matter>